Research Square

Preprints are preliminary reports that have not undergone peer review.
They should not be considered conclusive, used to inform clinical practice,
or referenced by the media as validated information.

Pseudomonas syringae pv. tomato DC3000, which acquired GI-1 from P. syringae pv. tabaci 6605 via horizontal gene transfer, exhibits increased virulence

Kotomi Kunishi
Okayama University
Norika Fujisawa
Okayama University
Yuta Watanabe
Okayama University
Yasuhiro Ishiga
University of Tsukuba
Hidenori Matsui
Okayama University
Nanami Sakata
Okayama University
Yoshiteru Noutoshi
Okayama University
Kazuhiro Toyoda
Okayama University
Yuki Ichinose
yuki@okayama-u.ac.jp

Okayama University

Research Article

Keywords: genomic island, horizontal gene transfer (HGT), integrative and conjugative element (ICE), pathogenicity island, Pseudomonas syringae, tabtoxin

Posted Date: November 24th, 2026

DOI: https://doi.org/10.21203/rs.3.rs-11744971/v1

License: This work is licensed under a Creative Commons Attribution 4.0 International License.
Read Full License

Additional Declarations: No competing interests reported.

Abstract

Pseudomonas syringae pv. tabaci 6605 (Pta6605) harbors a genomic island, GI-1, containing the tabtoxin biosynthesis genes cluster, which is essential for virulence because the loss of GI-1 in Pta6605 abolished the ability to cause severe disease symptoms when inoculated into host tobacco plants. GI-1 has tRNA Lys at the right border and ψtRNA Lys at the left border, and is known to be released from the chromosome at the tRNA Lys sites and circularize. Therefore, we attempted to transfer GI-1 into P. syringae pv. tomato DC3000 (PtoDC3000), which has two sequences of tRNA Lys identical to those of Pta6605. A kanamycin resistance (Km^R) gene was introduced into GI-1 as a selection marker, and following co-culture with PtoDC3000—which naturally exhibits rifampicin resistance (Rif^R)—strains displaying both Km^R and Rif^R phenotypes were selected. These strains were identified as PtoDC3000 that had acquired GI-1. GI-1 was preferentially integrated into T52 of PtoDC3000, an ortholog of tRNA Lys of GI-1. The PtoDC3000 that had acquired GI-1 produced tabtoxin, and induced early and more severe disease symptoms than the wild type of PtoDC3000 on the host A. thaliana. The enhancement of virulence resulting from GI-1 acquisition was particularly pronounced in PtoDC3000 strains that had lost the ability to produce coronatine. Although PtoDC3000 strains that had lost the ability to produce coronatine exhibited a markedly reduced ability to cause disease, the introduction of GI-1 resulted in a substantial recovery of virulence. These results indicate that GI-1 can be transferred horizontally to other bacterial species, contributing to the expansion of virulence.

Introduction

Pseudomonas syringae species are Gram-negative phytopathogenic bacteria that cause disease in a wide range of plant species. There are over 60 different pathogenic variants (pathovars) that differ in host plant species and the type of disease symptoms they cause (Xin et al. 2018). They often produce phytotoxins: tabtoxin is produced by *P. syringae* pv. *tabaci* (*Pta*) 6605, a causal agent of tobacco wild fire disease, and coronatine is produced by *P. syringae* pv. *tomato* (*Pto*) DC3000, a causal agent of bacterial speck on tomato and *Arabidopsis thaliana* (Bender et al. 1999; Watanabe et al. 2025). Tabtoxin is a monocyclic β-lactam, and its peptidase-digested metabolite, tabtoxinine-β-lactam induces chlorosis by inhibiting glutamine synthetase. Tabtoxin is produced not only in *Pta*, but also the oat pathogen pv. *coronafaciens*, coffee pathogen pv. *garcae*, and rice pathogen pv. *oryzae* (Arrebola et al. 2011; Bender et al. 1999). These pathovars are phylogenetically distant from one another, and it is believed that the ability to produce tabtoxin was acquired independently by horizontal gene transfer (HGT) rather than phylogenetically because not all pathovars in the same clade have the ability to produce tabtoxin (Hwang et al. 2005). In fact, the region adjacent to the tabtoxin biosynthetic genes cluster contains the integrase *xerC* and tRNA^{Lys} genes, which are often found near boundaries of genomic islands (GIs), likely the result of HGT (Kinscherf and Willis 2005; Watanabe et al. 2025).

Very recently, we found two GIs, GI-1 and GI-2, in *Pta*6605, a highly virulent and motile strain (Watanabe et al. 2025). Both GIs are dynamic, have a pseudogene of tRNA^{Lys} (ψtRNA^{Lys}) on the left border and an intact tRNA^{Lys} gene on the right border, and are excised at these tRNA^{Lys} sites. Released GIs are

circularized and seem to reintegrate to an original tRNA^{Lys} site (Watanabe et al. 2025). GIs are composed of “backbone (core) genes”, which are conserved across many GIs found in a wide range of bacterial species. They are responsible for the translocations and maintenance of GI and “cargo (accessory) genes”, which are components unique to each specific GI. The function transferred by each GI is determined by the cargo genes. GI-1 has three effector genes and a tabtoxin biosynthetic genes cluster. Deletion experiments revealed that GI-1 is an indispensable virulence factor to cause wild fire disease in tobacco (Watanabe et al. 2025). Among cargo genes, we recently revealed that tabtoxin biosynthetic genes in GI-1 are a dominant virulence factor (Kunishi et al. 2026).

In this study, we attempted to transfer GI-1 into *Pto*DC3000, which has two sequences of tRNA^{Lys} identical to those of *Pta*6605. A kanamycin resistance (Km^{r}) gene was introduced into GI-1 as a selection marker; meanwhile, because *Pto*DC3000 is naturally rifampicin-resistant (Rif^{r}), strains exhibiting both Km^{r} and Rif^{r} phenotypes were selected following coculture of the two strains. The *Pto*DC3000 that had acquired GI-1 was able to produce tabtoxin and cause significantly severer disease symptoms on *A. thaliana* than *Pto*DC3000 WT. To observe the effects of the acquisition of GI-1, we abolished the coronatine biosynthesis ability of *Pto*DC3000, thereby reducing its virulence. Specifically, we generated a mutant strain, Δ*cmaA*, deficient in coronatine biosynthesis and introduced GI-1 into it.

The Δ*cmaA* mutant strain showed markedly reduced ability to cause disease symptoms in *Arabidopsis* seedlings; however, the Δ*cmaA* strain harboring GI-1 resulted in a substantial recovery of its virulence in flood inoculation assays. Although coronatine and tabtoxin act on different sites, tabtoxin partially complemented the reduction of virulence associated with the loss of coronatine-producing ability. We discuss the potential for the dissemination of virulence genes mediated by GIs.

Materials and Methods

Bacterial strains and plasmids

The bacterial strains and plasmids used in this study are listed in Table S1. *Pta* and *Pto* strains were grown at 27°C in King's B (KB) medium supplemented with 25—50 μg/mL nalidixic acid (Nal), Rif, or Km as needed. *Escherichia coli* strains were grown at 37°C in Luria-Bertani (LB) medium supplemented with 50 μg/mL ampicillin or Km as needed.

Generation of GI-1-acquired PtoDC3000

*Pta*6605 has at least two GIs, GI-1 and GI-2 (Watanabe et al. 2025), and both have the potential for HGT. Therefore, to eliminate the possibility of GI-2 translocation, *Pta*6605 ΔGI-2 was used as a donor cell for GI-1 translocation. To obtain a *Pto*DC3000 that had acquired GI-1 from *Pta*6605, we used bacterial conjugation and selection with antibiotic resistance. The mobilizable plasmid vector, pARO191 (Parke 1990), which possesses the Km resistance gene (Km^{r}), was integrated into the GI-1 of *Pta*6605. To avoid any insertional effect of pARO191 on the function of GI-1, the integration site in GI-1 was selected to be

the spacer region between *Pta*6605_RS20485 (hereafter, we omit "*Pta*6605" from the gene locus) and RS28250 (Fig. S1A). Using the primers GI-1_u and GI-1_d, a 547 bp spacer region between RS20485 and RS28250 was amplified with GoTaq Green Master Mix (Promega, Tokyo, Japan), cloned into pGEM-T Easy (Promega), and finally inserted into pARO191 to obtain pARO-28250L. The pARO-28250L was introduced into *Pta*6605 ΔGI-2 using *E. coli* S17-1 strain by conjugation. The recipient bacterium, *Pto*DC3000, is spontaneously Rif resistant (Rif^r). *Pta*6605 ΔGI-2 (pARO-28250L) and *Pto*DC3000 WT were independently cultured overnight (o/n) in KB medium at 27℃ with appropriate antibiotics; then they were harvested by centrifugation, mixed with small amount of KB broth, and put on the sterilized nitrocellulose membrane on KB agar plates. After incubation o/n at 27℃, bacteria were suspended in KB broth and spread on KB plates with Rif (50 μg/ml) and Km (25—50 μg/ml). After two days of incubation, the colonies that appeared were candidates for GI-1-acquired *Pto*DC3000. *Pto*DC3000, which acquired a tabtoxin-defective GI-1, was also generated. Instead of pARO-28250L, a part of *tabA* open reading frame (RS20860) of *Pta*6605 was amplified by PCR with a primer pair (tab_E and tab_F) and finally inserted into pARO191 to obtain pARO191-*tabA* (Fig. S1B). The subsequent procedure was the same as for intact GI-1 translocation. All primers, plasmid DNA, and bacterial strains used in this study are listed in Tables S1 and S2.

PCR to distinguish Pta6605 and PtoDC3000

During the conjugation process, *Pta* may spontaneously acquire resistance to Rif, which can result in the appearance of colonies on KB agar medium containing both Km and Rif. Therefore, it is necessary to verify that any Km^r, Rif^r colonies are indeed *Pta*. PCR primers that amplify *hrpZ* (hrpZ and hrpZ_d) produce 726 bp in *Pto*DC3000, but only 331 bp in *Pta*6605 due to a spontaneous deletion of the central 331 bp of *hrpZ* (Taguchi et al. 2001). Furthermore, *cfa6*, one of the coronatine biosynthesis genes (Brooks et al. 2004), was amplified by 967 bp using primers (cfa6_u1 & cfa6_d1) in *Pto*DC3000 but not in *Pta*. PCR was carried out with 30 cycles using KOD One PCR Master Mix Blue (TOYOBO) with annealing at 68°C for *hrpZ* and 65°C for *cfa6* and extension for 5 s using a bacterial suspension as template DNA.

PCR detection of GI-1-specific DNA

To confirm that the entire GI-1 region had been transferred to *Pto*DC3000, we analyzed the presence of several GI-1-specific cargo genes by PCR. PCR-amplified DNA and primer information are shown in Fig. 1 and Table S2. PCR was carried out with 30 cycles using KOD One PCR Master Mix Blue with annealing at 63°C and extension for 5 s using a bacterial suspension as template DNA.

PCR to determine the integration site of GI-1

To identify the integration site of GI-1 in *Pto*DC3000, PCR was performed to generate PCR-amplified fragments when inserted into $tRNA^{Lys}$ of *Pto*DC3000 (PSPTO_t13 and PSPTO_t52). PCR using primers as shown in Fig. 2 was carried out with 30 cycles using KOD One PCR Master Mix Blue with annealing at

64°C and extension for 5 s using a bacterial suspension as template DNA. The amplified DNA was directly sequenced to confirm that it was the target DNA.

Detection of tabtoxin

Tabtoxin production was investigated by examining its growth-inhibitory activity against *E. coli*. It has been reported that tabtoxin production is significantly affected by growth conditions, specifically carbon sources, nitrogen sources, and amino acids (Dehbi et al. 2001). Therefore, to efficiently detect tabtoxin production, culture conditions were modified as follows: bacteria were incubated o/n in LB supplemented with 10 mM $MgCl_2$, then the culture medium was changed to an M9-based medium in which NH_4Cl (the nitrogen source) was replaced with 17 mM KNO_3, and glucose (the carbon source) was replaced with 2% sucrose for further o/n incubation according to the method of Dehbi et al. (2001). The bacteria harvested were adjusted to the concentration to OD_{600} = 5, and 20 µL of the bacterial suspension was absorbed onto a filter paper AAdisc (φ 6 mm, Advantec Toyo Kaisha, Ltd.), which was then placed on M9 medium seeded with *E. coli*. After 2 d incubation at 37°C, the growth inhibition zone of each bacterium was observed as an effect of tabtoxin.

Plant materials and inoculation procedure

To investigate the effect of GI-1 acquisition on virulence in *Pto*DC3000, inoculation tests were carried out using the host plant *A. thaliana* ecotype Colombia WT. Inoculation was performed according to the flood-inoculation method as described by Ishiga et al. (2017) with slight modification. Briefly, ethanol-sterilized seeds were sown on 1/2 Murashige and Skoog (MS) medium supplemented with 1% sucrose. After 2 wks incubation at 22°C with a 16-h photoperiod, seedlings were transplanted into new 1% sucrose 1/2 MS plates and grown for a further 5 d. The inoculum was prepared in 10 mM $MgSO_4$ at an OD_{600} of 0.002 to 0.02 (4×10^6 to 4×10^7 colony-forming units (CFU)/mL) supplemented with 0.025% (vol/vol) Silwet L77 (OSI Specialties, Danbury, CT) to promote cell attachment. Seedlings of *A. thaliana* were flooded by the inoculum for approximately 2 min. After the inoculum was decanted, the plates were incubated at 22°C. Photographs of seedlings were taken at 3, 5, and 7 dpi. To measure bacterial growth, two leaf discs (4 mm diameter) were collected at 3-h post inoculation (0 dpi) and 3 dpi and ground in 1 mL of sterile water. After serial dilutions, the suspension was spotted on KB agar medium with Rif. Following incubation at 27°C for 2 d, the resulting bacterial colonies were counted, and CFU was calculated.

Generation of coronatine biosynthesis-defective mutant in PtoDC3000

cmaA is reported to be required for coronatine production, and the virulence of the *cmaA* mutant of *Pto*DC3000 was remarkably reduced (Brooks et al. 2004; Ishiga et al. 2012). To construct a Δ*cmaA* mutant, the upstream region (*cmaE*) and downstream region (*cmaB*) of *cmaA* (Fig. S1C) were amplified using *Pto*DC3000 genomic DNA as a template and KOD One PCR Master Mix Blue. Annealing was performed at 65°C, and extension was carried out for 2 s. Using In-Fusion Snap Assembly Master Mix

(Takara Bio Inc., Kusatsu, Japan), both PCR products were connected and inserted into *Bam*HI-digested pKN (Kashihara et al. 2022) to generate pKN-Δ*cmaA*. The pKN-Δ*cmaA* was introduced into *E. coli* S17-1 and subsequently used for conjugation with the *Pto*DC3000 WT. The deletion mutant was generated by double homologous recombination as previously described (Kunishi et al. 2026). The candidates for Δ*cmaA* mutants were selected on KB medium supplemented with 12% sucrose to isolate deletion mutants by second homologous recombination. The Δ*cmaA* deletion mutant strains were confirmed by PCR and sequencing.

Coronatine bioassay

Since coronatine was known to induce marked hypertrophy in potato tuber tissues (Saeki et al. 1979), a bioassay was conducted following that method. Potato tuber slices approximately 8 mm thick were prepared, and the surface was touched by a toothpick bearing a colony of the test bacterium. Potato tuber slices were incubated at room temperature in the dark for 5 d, and the cut surfaces were photographed.

Statistical analysis of disease symptoms

To statistically analyze the severity of disease symptoms, typical symptoms were categorized into levels ranging from 0 to 4. Level 0 represents a state with no visible symptoms; level 1, a state where rosette leaves have begun to turn yellowish-green; level 2, a state where rosette leaves have turned yellow; level 3, a state where rosette leaves have withered and turned white, with only the shoot apex remaining green; and level 4, a state where the entire seedling, including the shoot apex, has turned white and died. Furthermore, the level of symptoms in the *Arabidopsis* inoculated with the respective bacterial strains was evaluated by calculating the mean values.

Results

Generation of PtoDC3000 conjugants acquiring GI-1

After conjugation, the cells were spread on Rif- and Km-containing KB plates, and a number of colonies were obtained after 2 days incubation. PCR amplification of the obtained colonies yielded a 726 bp *hrpZ* fragment and a 967 bp *cfa6* fragment, confirming them to be *Pto*DC3000 (Fig. S2).

Genetic dissection of GI-1-acquired PtoDC3000

In order to confirm the integration of GI-1 into *Pto*DC3000, GI-1-specific DNAs were amplified by PCR. The presence of DNA of RS28250, RS20590, RS20685 (*hopF1*), and RS20860 (*tabA*) was confirmed in *Pta*6605 WT and *Pto*DC3000 with GI-1 (#1 and #2) but not in *Pto*DC3000 WT (Fig. 1). These results indicate that the Km^r and Rif^r colonies are *Pto*DC3000 strains harboring the entire GI-1.

Analysis of integration sites of GI-1 $_{6605}$ in PtoDC3000

To identify the integration site of GI-1 in *Pto*DC3000, PCR analysis was carried out. Because two $tRNA^{Lys}$ sequences in *Pto*DC3000 (PSPTO_t13 and PSPTO_t52) are identical to those in *Pta*6605, we predicted that GI-1 might be transferred into t13 or t52 of *Pto*DC3000. As shown in Fig. 2, the DNA status of each bacterium was analyzed by PCR using two primer combinations in *Pta*6605 WT, *Pto*DC3000 WT, and transconjugants of GI-1-acquired *Pto*DC3000. The absence of DNA band in lanes 1 and 2 indicates that GI-1 at t13 was not integrated in all bacterial strains, and the DNA bands in lane 3 and lane 6 indicate no integration or release of GI-1 at t13 and t52, respectively. The DNA bands in lanes 4 and 5 mean the integrations of GI-1 at t52 in the transconjugants. Furthermore, the DNA band in lane 7 indicates circularization of GI-1 in *Pta*6605 WT and GI-1-acquired *Pto*DC3000. In *Pto*DC3000, t13 and t52 are orthologs of RS24860 (a $tRNA^{Lys}$ gene located near *clpB*) found at the right border of GI-2 in *Pta*6605 and RS20895 (a $tRNA^{Lys}$ gene adjacent to *queC*) found at the right border of GI-1 in Pta6605, respectively. This suggests that GI-1 may preferentially integrate into t52, which is the ortholog of RS20895 (located at the right border of GI-1).

Tabtoxin production

Because it has already been shown that the hypervirulence of *Pta*6605 is due in part to its ability to produce tabtoxin (Kunishi et al. 2026), tabtoxin production of the GI-1-acquired *Pto*DC3000 was investigated. Tabtoxin is a non-specific phytotoxic dipeptide, and its peptidase-digested metabolite, tabtoxinine-β-lactam, inhibits glutamine synthetase, leading to an abnormal accumulation of ammonia and a glutamine deficiency. When the test bacteria were placed on a paper disc on a culture medium embedded with *E. coli* and incubated at 37°C for two days, a large growth inhibition zone appeared around *Pta*6605 WT, and a small but definite growth inhibition zone was observed around GI-1-acquired *Pto*DC3000. These growth inhibition zones disappeared when glutamine was added to the culture medium, indicating that this was due to the action of tabtoxin (Fig. 3). Consequently, the GI-1-acquired *Pto*DC3000 was able to produce tabtoxin, although the amount produced was lower than that of *Pta*6605.

Virulence of GI-1-acquired PtoDC3000

The virulence of *Pto*DC3000 strains was investigated by the flood inoculation method. Seedlings of *A. thaliana* were inoculated with *Pto*DC3000 WT, GI-1-acquired *Pto*DC3000, or *tabA*-mutated GI-1-acquired *Pto*DC3000 at bacterial concentrations of OD_{600} = 0.002 (Fig. 4). All *Arabidopsis* seedlings inoculated were yellowed and finally withered. Most of the rosette leaves of *A. thaliana* inoculated with *Pto*DC3000 WT began to turn yellowish-green at 3 dpi, and turned yellow by 5 dpi. Furthermore, by 7 dpi the entire plant except for the shoot apex turned white. In contrast, *Arabidopsis* plants inoculated with GI-1-acquired *Pto*DC3000 exhibited a more rapid progression of symptoms: the rosette leaves whitened quickly, and the entire plant including the shoot apex turned white by 7 dpi. On the other hand, in *A. thalinana* inoculated with *tabA*-mutated GI-1-acquired *Pto*DC3000, the symptom progression was comparable to, or even slightly slower than, that observed with the *Pto*DC3000 WT inoculation. To compare the level of bacterial virulence, disease symptoms of each inoculated seedling were scored on

a scale of 0 to 4, in accordance with the criteria described in the Materials and Methods (Fig. 4B), and the symptoms of all inoculated individuals were evaluated (Fig. 4C). Symptom progression was most rapid following inoculation with GI-1-acquired *Pto*DC3000, whereas the progression was slower following inoculation with the *Pto*DC3000 WT and *tabA*-mutated GI-1-acquired *Pto*DC3000. Additionally, disease symptoms progressed more rapidly at higher inoculation concentrations. Compared to the inoculation at a bacterial concentration of OD_{600} = 0.002, disease symptoms progressed more rapidly when inoculated at OD_{600} = 0.02 (Fig. S3).

Virulence of coronatine-defective PtoDC3000 and its GI-1-acquired strain

To clearly observe changes in virulence resulting from the acquisition of the ability to produce tabtoxin, we generated a coronatine-deficient mutant of *Pto*DC3000 (Δ*cmaA*), introduced GI-1 into this Δ*cmaA* strain (which exhibits reduced virulence), and evaluated its virulence. The loss of the capability to produce coronatine was confirmed by the loss of hypertrophic activity in potato tuber tissue (Fig. S4). The inoculation was performed at an OD_{600} of 0.002. Symptom development of the *Arabidopsis* inoculated with Δ*cmaA* was largely delayed compared to the inoculation with *Pto*DC3000 WT (Fig. 4). The GI-1-acquired Δ*cmaA* resulted in the partial recovery of virulence, although it did not reach WT level. However, *tabA*-mutated GI-1-acquired Δ*cmaA* didn't alter virulence, confirming the tabtoxin production is a key factor in GI-1. To statistically evaluate disease severity, the mean values for each inoculation group were plotted over time (Figs. 4D and S3C). After inoculation at an OD_{600} of 0.002, the GI-1-acquired *Pto*DC3000, which produces tabtoxin in addition to coronatine, exhibited significantly more severe disease symptoms at 5 and 7 dpi than the other inoculated groups. Next in severity were *Pto*DC3000 WT and the *tabA*-mutated GI-1-acquired *Pto*DC3000, both of which produce coronatine. These were followed by the GI-1-acquired Δ*cmaA* strain, which produces tabtoxin. The mildest symptoms were observed in the Δ*cmaA* and *tabA*-mutated GI-1-acquired Δ*cmaA* strains, neither of which produces either toxin. The result showing that the GI-1-acquired *Pto*DC3000, which produces both coronatine and tabtoxin, induced more severe and rapid symptoms than *Pto*DC3000 WT strain was similarly confirmed even when inoculation was performed at an OD_{600} of 0.02 (Fig. S3C).

Bacterial growth and toxin production

Following inoculation at an OD_{600} of 0.002, bacterial growth levels were examined. Bacterial growth of *Pto*DC3000 WT, GI-1-acquired *Pto*DC3000, and *tabA*-mutated GI-1-acquired *Pto*DC3000 was significantly higher than that of Δ*cmaA*, GI-1-acquired Δ*cmaA*, and *tabA*-mutated GI-1-acquired Δ*cmaA* (Fig. 5). These results indicate that while the ability to produce tabtoxin does not affect bacterial growth, the production of coronatine provides an advantage for bacterial growth.

Discussion

Through HGT, bacteria can acquire new genes that enable adaptation to novel environments. These include genes involved in symbiosis and pathogenesis and resistance to antibiotics, metals, and toxins,

as well as the production of secondary metabolites, including toxins. The mechanisms of HGT can be classified into three well-studied types: 1) transformation, the natural take up of exogenous DNA from the environment, 2) transduction, the transfer of DNA by bacteriophages, and 3) conjugation, the contact-dependent DNA transfer from donor cells to recipient cells via a conjugation apparatus such as type IV pili (Johnson and Grossman 2015). Recently, a large family of integrative and conjugative elements (ICEs, also called conjugative transposons) were found as mobile DNA elements in many bacteria (Wozniak and Waldor 2010).

In phytopathogenic bacteria, ICEs have long been identified through extensive genome analysis, and genes potentially influencing virulence and fitness—such as type III effector (T3E) genes, toxin genes, and drug resistance genes—have been found in cargo genes (de Assis et al. 2022). For example, PPHGI-1 which carries the avirulence gene *avrPphB* in *Pseudomonas syringae* pv. *phaseolicola* strain 1302A and PAPI-1 in *P. aeruginosa* strain PA14 were discovered more than two decades ago (Pitman et al. 2005; He et al. 2004). ICEs in *P. syringae* pv. *actinidiae* carry a copper resistance gene (Colombi et al. 2017). PmaICE-DQ in *P. syringae* pv. *maculicola* ES4326, which contains multiple TSE genes, was found to be excised and conjugated across strains (Baltrus et al. 2022), and GI-1 in *P. syringae* pv. *tabaci* 6605 carry tabtoxin biosynthesis genes cluster and T3E genes (Watanabe et al. 2025). Furthermore, HAI2 in *Pectobacterium atrosepticum* SCRI1043 carries genes for coronafacic acid (CFA) biosynthesis gene cluster (Panda et al. 2016), and *Xanthomonas campestris* pv. *campestris* CFBP 9145 carries T3E genes and copper resistance genes in ICEs (Boyer et al. 2024). In general, ICEs are integrated into the chromosome of the host bacterium, and their transfer requires the following three stages: 1) excision from the chromosome, 2) transfer of the excised DNA or a copy thereof, and 3) integration into the chromosome of the recipient cell. While there are many analyses of genomic sequences thought to be ICEs, these studies have merely identified the presence of DNA elements presumed to have undergone transposition (de Assis et al. 2022). There are not many bacteria for which HGT has experimentally been confirmed in the laboratory. PPHGI-1 from *P. syringae* pv. *phaseolicola* 1302A, which carries the avirulence gene *avrPphB*, could be transferred to *P. syringa*e pv. *phaseolicola* 1448A in plant leaves; consequently, *Pph*1448A became avirulent toward its original compatible bean host cultivar Tendergreen (Lovell et al. 2009). While PAPI-1 from hypervirulent *P. aeruginosa* PA14 was reported to be transferred to a hypovirulent *P. aeruginosa* PAO1 strain (Qiu et al. 2006; Carter et al. 2010). In PAPI-1, 19 ORFs were reported to be necessary for virulence toward *A. thaliana* and mouse (He et al. 2004). It would be expected that transconjugants which have acquired PAPI-1 would exhibit increased virulence; however, no such reports currently exist. Therefore, this is a first report that virulence was enhanced via HGT. Does the transmission of GI-1 from *Pta* to *Pto* actually occur in nature? Since these bacteria do not share a common host plant, the likelihood of this happening is presumed to be extremely low. However, the findings of this study are not limited solely to the transfer of DNA from *Pta* to *Pto*. *Pto*DC3000 was used as a representative bacterium of *Pseudomonas*. Since the sequence of the $tRNA^{Lys}$ is highly conserved not only among strains of *P. syringae* strains but also across different species within the genus *Pseudomonas*, it is conceivable that GI-1 could be transferred to *Pseudomonas* bacteria as well as to other strains of *P. syringae*.

Similar to tabtoxin, the ability to produce coronatine is also distributed independently of phylogenetic classification (Hwang et al. 2005). Coronatine is known to be produced by pathovars of *Pseudomonas syringae* such as *tomato*, *glycinea*, and *maculicola*; however, not all isolates belonging to these pathovars produce coronatine (Hwang et al. 2005). It is thought that these isolates either lost the ability to produce toxins after having acquired it or that individual isolates acquired this capability independently. Similar findings have been obtained for other toxins produced by *Pseudomonas syringae*, such as phaseolotoxin. It has been suggested that the ability to produce phaseolotoxin, one of the toxins produced by *P. syringae*, was acquired via HGT (Sawada et al. 2002). Coronatine has two distinct components: the polyketides coronafacic acid (CFA) and coronamic acid (CMA). As described above, *Pectobacterium atrosepticum* SCRI1043, a causal agent of blackleg disease of potato, carries genes for CFA biosynthesis in the horizontally acquired island 2 (HAI2). The deletion of HAI2 resulted in the attenuation of blackleg symptoms in potato stems, indicating that CFA is an important virulence factor for this disease (Panda et al. 2016).

The ability to produce tabtoxin was conferred on *Pto*DC3000 by introducing GI-1. However, the level of tabtoxin production by *Pto*DC3000 was markedly lower than that by *Pta*6605 (Fig. 3). It is presumed that this is due to factors such as an insufficient supply of tabtoxin precursors in *Pto*DC3000 or the absence of signals required to activate production. In addition to the *Pto*DC3000 WT strain, we generated five mutant strains with altered toxin-producing capabilities as summarized in Table S3. The WT and WT + GI-1 (*tabA*$^{-}$) strains produced only coronatine, whereas the WT + GI-1 strain produced both coronatine and tabtoxin. In contrast, the Δ*cmaA* and Δ*cmaA* + GI-1 (*tabA*$^{-}$) strains produced neither toxin, while the Δ*cmaA* + GI-1 strain produced only tabtoxin. Among these *Pto*DC3000 strains, the WT + GI-1 strain, which produced both toxins, induced disease symptoms most rapidly, followed by the coronatine-producing WT and WT + GI-1 (*tab*$^{-}$) strains. The Δ*cmaA* + GI-1 strain, which produced only tabtoxin, induced symptoms faster than the strains producing neither toxin (Δ*cmaA* and Δ*cmaA* + GI-1 (*tabA*$^{-}$)) but did not reach WT levels. This is thought to be due to the low level of tabtoxin production in *Pto*DC3000. It has been revealed that tabtoxin can function as a substitute for coronatine, despite having a completely different mechanism of action.

Conclusion

Strain *Pta*6605 harbors GI-1, an ICE containing the genes cluster responsible for tabtoxin production. GI-1 is inserted into the $tRNA^{Lys}$ gene of strain *Pta*6605 and was horizontally transferred during co-culture to strain *Pto*DC3000, which possesses an identical $tRNA^{Lys}$ sequence. The GI-1-acquired *Pto*DC3000 strain produced tabtoxin, but the production level was considerably lower than that of *Pta*6605. This suggests that *Pto*DC3000 may lack the necessary precursors or activation conditions necessary for tabtoxin biosynthesis. The GI-1-acquired *Pto*DC3000 strain induced disease symptoms more rapidly than the *Pto*DC3000 WT strain, probably due to the additional production of tabtoxin. This enhancement of virulence resulting from tabtoxin production became more apparent when GI-1 was introduced into a coronatine-defective mutant strain, Δ*cmaA*. The virulence of Δ*cmaA* was significantly reduced, and

introduction of GI-1 into the strain resulted in a partial recovery, although it did not reach the level of the WT strain. Consequently, the order of virulence among these strains is WT + GI-1 > WT > Δ*cmaA* + GI-1 > Δ*cmaA*. In terms of toxin production capabilities, this order corresponds to tabtoxin + coronatine > coronatine > tabtoxin > none. Given the sequence of the $tRNA^{Lys}$ is highly conservedwithin the genus *Pseudomonas*, it is conceivable that GI-1 from *Pta*6605 could be transferred not only to *Pto*DC3000 but also to other *Pseudomonas* including *P. syringae* strains.

Declarations

Conflict of interest

All authors declare no competing interests.

Ethical approval

This article does not contain any studies with human participants or animals performed by any of the authors.

Funding

This work was supported by JSPS KAKENHI Grant Number 26K08819 to Y.I.

Author Contribution

Conceptualization, Y.Ic.; methodology, Y.Ic.; formal analysis, K.K., N.F., Y.W., Y.Is.; investigation, K.K., N.F., Y.W.; curation, Y.Ic., Y.W.; writing, Y.Ic.; supervision, H.M., N.S., Y.N., K.T.; project administration, Y.Ic.; funding acquisition, Y.Ic.

Data availability

The data presented in this study are available on request from the corresponding author.

References

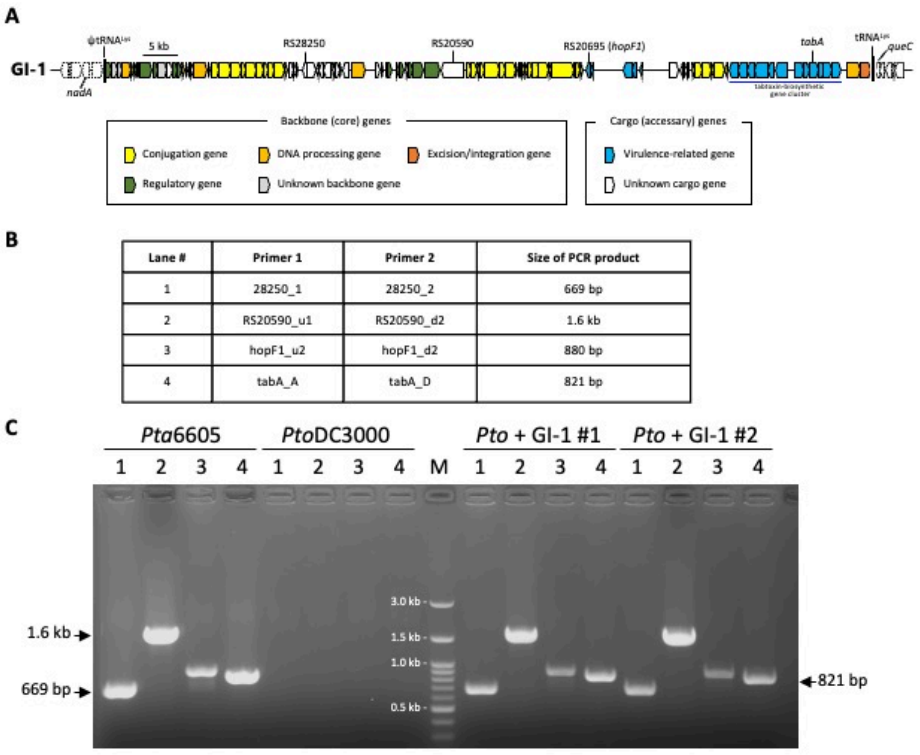
1. Arrebola E, Cazorla FM, Pérez-García A et al (2011) Genes involved in the production of antimetabolite toxins by *Pseudomonas syringae* pathovars. Genes 2:640–660. https://pmc.ncbi.nlm.nih.gov/articles/PMC3927611/
2. Baltrus DA, Feng Q, Kvitko BH (2022) Genome context influences evolutionary flexibility of nearly identical type III effectors in two phytopathogenic Pseudomonads. Front Microbiol 13. https://doi.org/10.3389/fmicb.2022.826365

3. Bender C, Alarcón-Chaidez F, Gross D (1999) *Pseudomonas syringae* phytotoxins: mode of action, regulation, and biosynthesis by peptide and polyketide synthetases. Microbiol Mol Biol Rev 63:266–292. https://doi.org/10.1128/mmbr.63.2.266-292.1999
4. Boyer C, Lefeuvre P, Richard D et al (2024) Complete genome sequence of a copper-resistant *Xanthomonas campestris* pv. *campestris* strain isolated from broccoli in Mauritius suggests adaptive gene gain through horizontal gene transfer. Phytopathology 114: 328–333. https://doi.org/10.1094/PHYTO-05-23-0177-SC
5. Brooks DM, Hernández-Guzmán G, Kloek AP et al (2004) Identification and characterization of a well-defined series of coronatine biosynthetic mutants of *Pseudomonas syringae*pv. *tomato*DC3000. Mol Plant-Microbe Interact 17: 162–174. https://doi.org/10.1094/MPMI.2004.17.2.162
6. Carter MQ, Chen J, Lory S (2010) The *Pseudomonas aeruginosa* pathogenicity island PAPI-1 is transferred via a novel type IV pilus. J Bacteriol 192:3249–3258. https://doi.org/10.1128/jb.00041-10
7. Colombi E, Straub C, Künzel S et al (2017) Evolution of copper resistance in the kiwifruit pathogen *Pseudomonas syringae* pv. *actinidiae* through acquisition of integrative conjugative elements and plasmids. Environ Microbiol 2:819–832. https://doi.org/10.1111/1462-2920.13662
8. Colombi E, Bertels F, Doulcier G et al (2024) Rapid dissemination of host metabolism–manipulating genes via integrative and conjugative elements. Proc Nat Acad Sci USA 121:e2309263121. https://doi.org/10.1073/pnas.2309263121
9. de Assis JCS, Gonçalves OS, Fernandes AS et al (2022) Genomic analysis reveals the role of integrative and conjugative elements in plant pathogenic bacteria. Mob DNA 13:19. https://doi.org/10.1186/s13100-022-00275-1
10. Dehbi F, Harzallah D, Larous L (2001) Effects of nutritional factors on production of tabtoxin, a phytotoxin, by *Pseudomonas syringae* pv. *tabaci*. Med Fak Landbouww Univ Gent 66:241–247
11. He J, Baldini RL, Déziel E et al (2004) The broad host range pathogen *Pseudomonas aeruginosa*strain PA14 carries two pathogenicity islands harboring plant and animal virulence genes. Proc. Nat. Acad. Sci. USA 101: 25302535. https://doi.org/10.1073/pnas.0304622101
12. Hwang MSH, Morgan RL, Sarkar SF et al (2005) Phylogenetic characterization of virulence and resistance phenotypes of *Pseudomonas syringae*. Appl Environ Microbiol 71:5182–5191. https://doi.org/10.1128/AEM.71.9.5182-5191.2005
13. Ishiga Y, Ishiga T, Ichinose Y et al (2017) *Pseudomonas syringae* flood-inoculation method in *Arabidopsis*. Bioprotocol 7:02. https://bio-protocol.org/en/bpdetail?id=2106&type=0
14. Ishiga Y, Ishiga T, Wangdi T et al (2012) NTRC and chloroplast-generated reactive oxygen species regulate *Pseudomonas syringae* pv. *tomato* disease development in tomato and *Arabidopsis*. Mol Plant-Microbe Interact 25:294–306. https://doi.org/10.1094/MPMI-05-11-0130
15. Johnson CM, Grossman AD (2015) Integrative and conjugative elements (ICEs): what they do and how they work. Annu Rev Genet 49:577–601. https://doi.org/10.1146/annurev-genet-112414-055018

16. Kashihara S, Nishimura T, Noutoshi Y et al (2022) HopAZ1, a type-III effector of *Pseudomonas amygdali* pv. *tabaci*, induces a hypersensitive response in tobacco wildfire-resistant *Nicotiana tabacum* 'N509'. Mol Plant Pathol 23:885–894. https://doi.org/10.1111/mpp.13198
17. Kinscherf TG, Willis DK (2005) The biosynthetic gene cluster for the β-lactam antibiotic tabtoxin in *Pseudomonas syringae*. J Antibiot 58:817–821. https://doi.org/10.1038/ja.2005.109
18. Kunishi K, Fujisawa N, Matsui H et al (2026) Tabtoxin biosynthetic gene cluster in *Pseudomonas syringae* pv. *tabaci* 6605 genomic island 1 (GI-$1_{Pta6605}$) is required for severe disease symptoms. J Gen Plant Pathol 92:166–170. https://doi.org/10.1007/s10327-026-01275-2
19. Lovell HC, Mansfield JW, Godfrey SAC et al (2009) Bacterial evolution by genomic island transfer occurs via DNA transformation in planta. Curr Biol 19:1586–1590. https://doi.org/10.1016/j.cub.2009.08.018
20. Panda P, Vanga BR, Lu A et al (2016) *Pectobacterium atrosepticum* and *Pectobacterium carotovorum* harbor distinct, independently acquired integrative and conjugative elements encoding coronafacic acid that enhance virulence on potato stems. Front Microbiol 7:397. https://doi.org/10.3389/fmicb.2016.00397
21. Parke D (1990) Construction of mobilizable vectors derived from plasmids RP4, pUC18 and pUC19. Gene 93:135–137. https://doi.org/10.1016/0378-1119(90)90147-J
22. Pitman AR, Jackson RW, Mansfield JW et al (2005) Exposure to host resistance mechanisms drives evolution of bacterial virulence in plants. Curr Biol 15:2230–2235. https://doi.org/10.1016/j.cub.2005.10.074
23. Qiu X, Gurkar AU, Lory S et al (2006) Interstrain transfer of the large pathogenicity island (PAPI-1) of *Pseudomonas aeruginosa*. Proc Natl Acod Sci USA 103:19830–19835. https://doi.org/10.1073/pnas.0606810104
24. Saeki R, Nishiyama K, Ichihara A et al (1979) Studies on the mechanism of physiological activity of coronatine effect of coronatine on cell wall extensibility and expansion of potato tuber tissue. Ann Phytopath Soc Japan 45:645–653. https://www.jstage.jst.go.jp/article/jjphytopath1918/45/5/45_5_645/_pdf/-char/en
25. Sawada H, Kanaya S, Tsuda M et al (2002) A phylogenomic study of the OCTase genes in *Pseudomonas syringae* pathovars: the horizontal transfer of the *argK-tox* cluster and the evolutionary history of OCTase genes on their genomes. J Mol Evol 54:437–457
26. https://link.springer.com/article/10.1007/s00239-001-0032-y
27. Taguchi F, Tanaka R, Kinoshita S et al (2001) $Harpin_{Psta}$from *Pseudomonas syringae*pv. *tabaci*is defective and deficient in its expression and HR-inducing activity. J Gen Plant Pathol 67:116–123. https://link.springer.com/article/10.1007/PL00012997
28. Watanabe Y, Kunishi K, Matsui H et al (2025) Genomic islands of *Pseudomonas syringae*pv. *tabaci*6605: Identification of *Pta*GI-1 as a pathogenicity island with effector genes and a tabtoxin cluster. Mol Plant Pathol 26: e70087. https://doi.org/10.1111/mpp.70087

29. Wozniak RAF, Waldor MK (2010) Integrative and conjugative elements: mosaic mobile genetic elements enabling dynamic lateral gene flow. Nat Rev Microbiol 8:552–563. https://doi.org/10.1038/nrmicro2382
30. Xin X-F, Kvitko B, He SH (2018) *Pseudomonas syringae*: what it takes to be a pathogen. Nat Rev Microbiol 16:316–328. https://pmc.ncbi.nlm.nih.gov/articles/PMC5972017/pdf/nihms969360.pdf

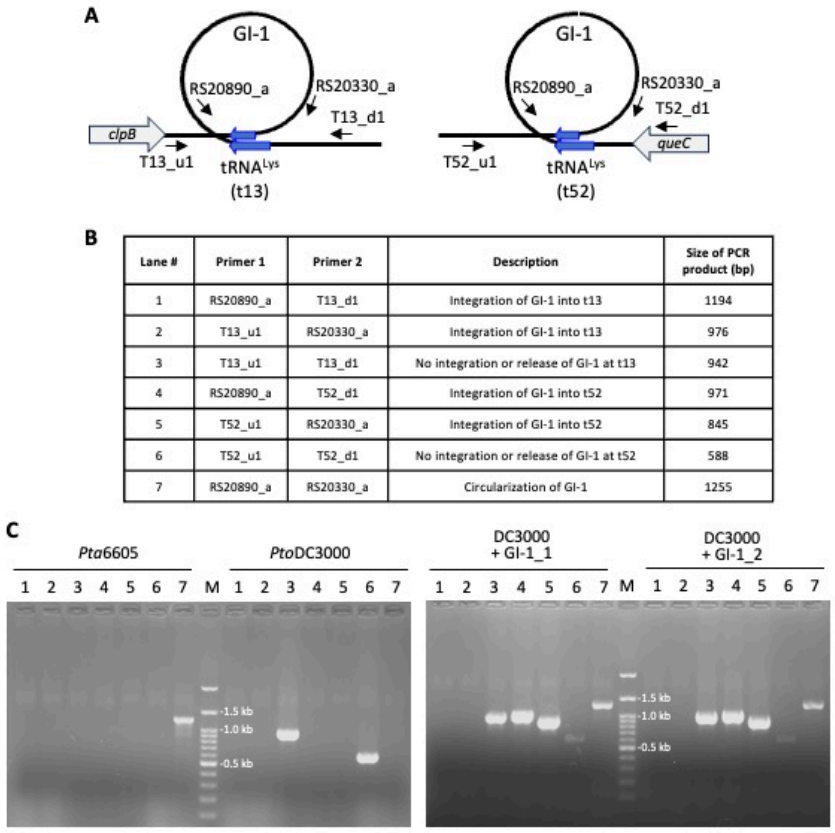
Figures



Lane #	Primer 1	Primer 2	Size of PCR product
1	28250_1	28250_2	669 bp
2	RS20590_u1	RS20590_d2	1.6 kb
3	hopF1_u2	hopF1_d2	880 bp
4	tabA_A	tabA_D	821 bp

Figure 1

PCR analysis of GI-1 in *Pto*DC3000 WT and Km- and Rif-resistant *Pto*DC3000 obtained by conjugation. The presence of GI-1-specific DNA in Km- and Rif-resistant *Pto*DC3000 was confirmed by PCR. **A** PCR-amplified regions are indicated above the model of GI-1. Genes are shown as pentagons. Putative function of core gene products and cargo gene product is shown in different colors. **B** Primer combinations used in PCR and sizes of PCR products. **C**Results of electrophoresis of PCR products.



B

Lane #	Primer 1	Primer 2	Description	Size of PCR product (bp)
1	RS20890_a	T13_d1	Integration of GI-1 into t13	1194
2	T13_u1	RS20330_a	Integration of GI-1 into t13	976
3	T13_u1	T13_d1	No integration or release of GI-1 at t13	942
4	RS20890_a	T52_d1	Integration of GI-1 into t52	971
5	T52_u1	RS20330_a	Integration of GI-1 into t52	845
6	T52_u1	T52_d1	No integration or release of GI-1 at t52	588
7	RS20890_a	RS20330_a	Circularization of GI-1	1255

Figure 2

Analysis of the integration site of GI-1 in *Pto*DC3000 and its circularization. **A** Model for the integration of GI-1 into T13 and T52 of *Pto*DC3000. The thick blue arrows are $tRNA^{Lys}$ genes and its pseudogenes. Black arrows indicate positions and directions of PCR primers. **B** Primer combinations used in PCR and size of PCR products. **C** Results of electrophoresis of PCR products.

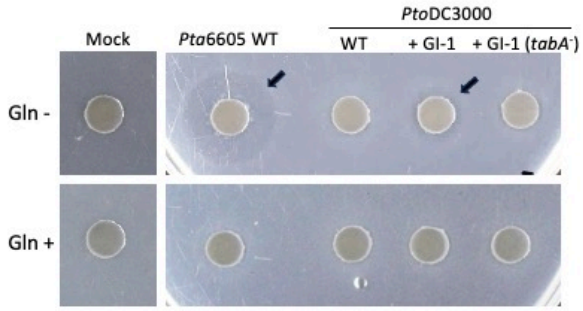


Figure 3

Tabtoxin production. Tabtoxin bioassay was performed using *E. coli* DH5α as the indicator bacterium. The test strains are *Pta*6605 WT, *Pto*DC3000 WT, GI-1-acquired *Pto*DC3000, and *tabA*-mutated GI-1-acquired *Pto*DC3000. *E. coli* suspension was mixed into MG soft agar medium and poured onto the plates. Then, filter paper discs, each loaded with 20 µL of culture medium containing either the *Pta*6605 WT strain or *Pto*DC3000 strains, were placed on the agar. Gln+ and Gln− indicate the presence (34 µM at

final concentration) or absence of glutamine in the medium. Photographs were taken after 48 h of incubation at 37°C and representative results obtained from two independent experiments. Arrows indicate the growth inhibition zone.

Fig. 4

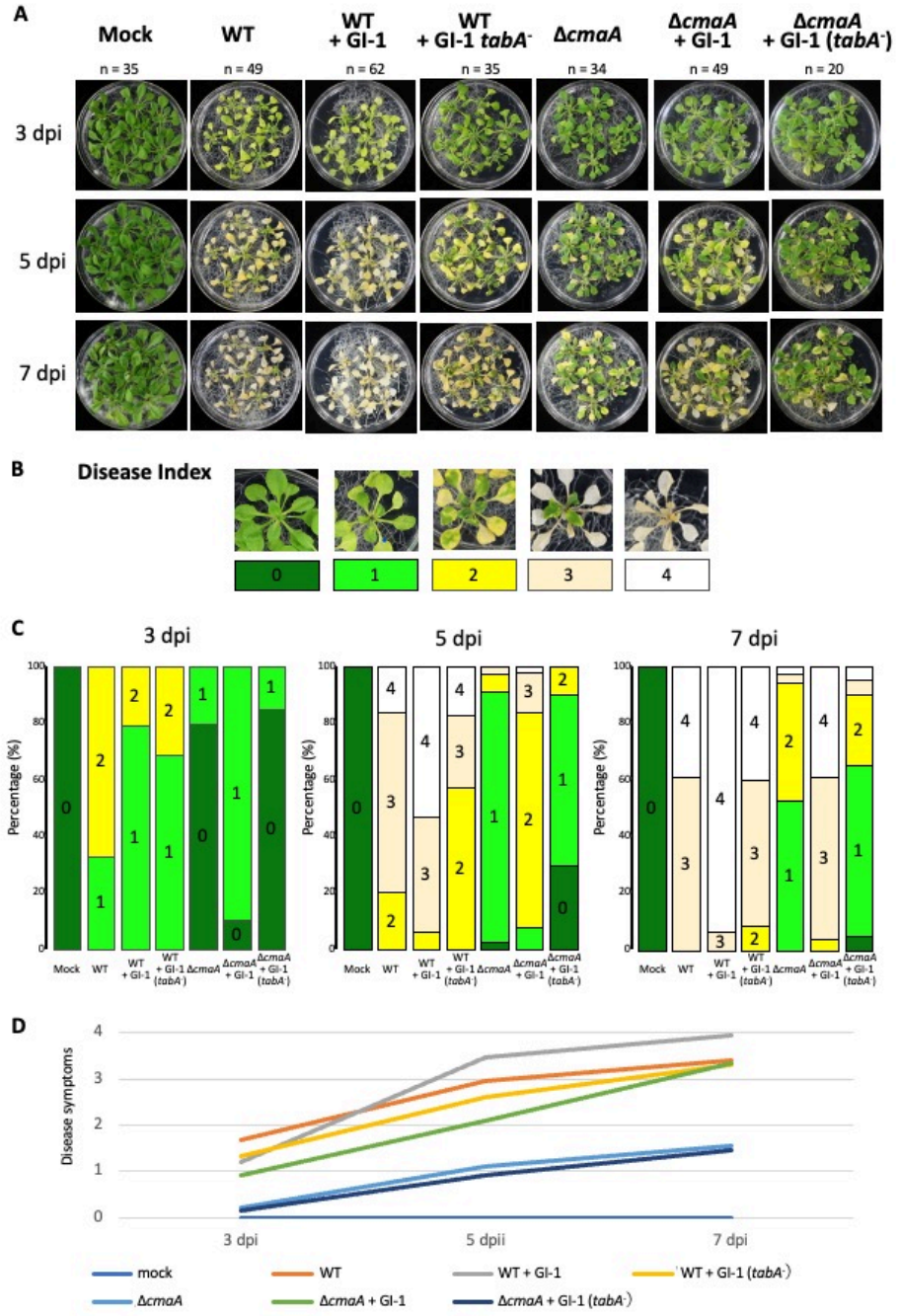


Figure 4

Virulence of each *Pto*DC3000 strain. *Arabidopsis* Col-0 WT was flood inoculated with *Pto*DC3000 WT, GI-1-acquired *Pto*DC3000, and *tabA*-mutated GI-1-acquired *Pto*DC3000, *Pto*DC3000 Δ*cmaA*, GI-1-acquired *Pto*DC3000 Δ*cmaA*, and *tabA*-mutated GI-1-acquired *Pto*DC3000 Δ*cmaA* at the bacterial density of 4×10^6 CFU/mL (OD_{600} = 0.002). **A** Typical phenotypes of *A. thaliana* inoculated with each bacterial strain. **B** Evaluation of disease symptoms. As described in Materials and Methods, the level of disease symptoms was classified as level 0 to 4. **C** Disease symptoms on at least 20 individual plants were scored at 3, 5 and 7 dpi. Each level of disease symptom is shown as a percentage. **D** Temporal progression of disease symptoms. Bacteria (*Pto*DC3000 WT, GI-1-carrying *Pto*DC3000, *tabA*-mutated GI-1-carrying *Pto*DC3000, *Pto*DC3000 Δ*cmaA*, GI-1-carrying *Pto*DC3000 Δ*cmaA*, and *tabA*-mutated GI-1-carrying *Pto*DC3000 Δ*cmaA*) were inoculated at a density of 4×10^6 CFU/mL (OD_{600} = 0.002).

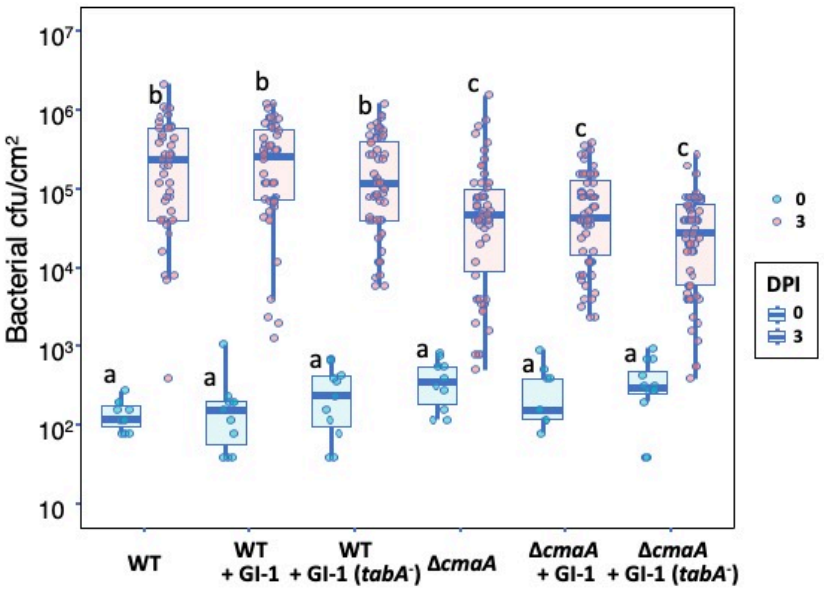


Figure 5

Bacterial growth in inoculated *Arabidopsis* leaves. Bacterial populations after flood inoculations (4×10^6 CFU/ml) were counted at 0 dpi (3 hpi) and 3 dpi. Bars represent standard errors from 4 independent experiments. Bacterial CFUs from 3 individuals for each strain in one experiment were pooled, and illustrated in a boxplot. Boxes show upper and lower quartiles of the data, and black lines represent the medians. Each dot represents raw data. *n* indicates the total number of biological replicates. Different

letters indicate statistically significant differences between groups (Kruskal–Wallis test followed by Dunn's multiple comparisons test with Benjamini–Hochberg correction, $p < 0.05$).

Supplementary Files

This is a list of supplementary files associated with this preprint. Click to download.

- FigureS1.jpeg
- FigureS2.jpeg
- FigureS3.jpeg
- FigureS4.jpeg
- TableS1.docx
- TableS2.docx
- TableS3.docx